*ISET Journal of Earthquake Technology, Paper No. 536, Vol. 54, No. 2-4, June-Dec. 2017, pp. 47-55*

# THE EFFECT OF COLUMN WALL THICKNESS ON THE SEISMIC PERFORMANCE OF NEW BOLT JOINTS

HE Mingsheng, LIU Li, WANG Jing and CHEN Lifu

College of Hydraulic and Civil Engineering
Shihezi University, Shihezi, Xinjiang 832003, China

**ABSTRACT**

A connection method of the beam-column joint of a new type of full bolt is proposed in this paper, which can be used to conveniently connect the square steel column with the H-shaped steel beam by full bolt. Pseudo-static test is carried out on two beam and column joints to study their bearing capacity, hysteresis performance, skeleton curve, ductility performance and energy dissipation capacity, and to study the influence of the column wall thickness of the joint area on its seismic performance. The study shows that the column wall thickness in the joint area has a significant impact on the failure form and the seismic performance. As the thickness of the column wall increases, the bearing capacity, ductility, stiffness and energy dissipation performance of the joint increase significantly. As for the connection method of the new joint, when the thickness of the column wall is different, its failure form is different, but its seismic performance, such as ductility and energy dissipation capacity, is better.

**KEYWORDS:** Square Steel Tube, Full-bolt Joint, Seismic Performance, Column Wall Thickness

## INTRODUCTION

The beam–column connection significantly affects the bearing capacity, deformation capacity and seismic performance of a structure. Typical welded steel frame connections in the California seismic belt failed to provide the expected ductility behavior, which was a result of the 1994 northridge earthquake in Los Angeles, California. The failure occurred at the joint of the beam, including full penetration weld fractures. Bolt joints have been used for decades and have performed well in past earthquakes. The existing research mainly focuses on high-strength T-shaped joints[1-4] adopted in H-shaped steel columns and H-shaped steel beams. Box columns are often used in high seismic hazard areas because of their good resistance to bidirectional bending. However, only a few researchers have developed and tested high strength bolts adopted in H-shaped steel beams and box columns[5-8].

A novel type of joint that is suitable for H-shaped beam and box column is proposed in this paper. The joint structure is simple and its bearing capacity is reasonable, which makes up for the disadvantages of traditional nodes: slow construction speed and poor on-site welding quality. The beam and column joints are composed of box column and H-shaped beam, and the side plate and beam end plate of the column are connected on site by high-strength bolt without nut, and the thread is directly made on the side plate of box column. This structure is shown in Figure 1. Box column and H-shaped beam are connected by high strength bolt, which contributes to quick and economic assembling on site. In order to estimate the ultimate tensile strength of high strength bolts without nuts, in the preliminary study of this project, the relevant force mechanism and experimental research were carried out with the parameters of plate thickness, thread shape, plate strength and bolt diameter[9, 10]. The results showed that the wall thickness of the column was an important factor in the bearing capacity of the new bolt joints.

Through the pseudo-static loading test, this paper studied the influence of the wall thickness of the joint area on its seismic performance when the new single-sided bolt joint is used for square steel pipe columns and steel beam joints, which provides a reference for further research.

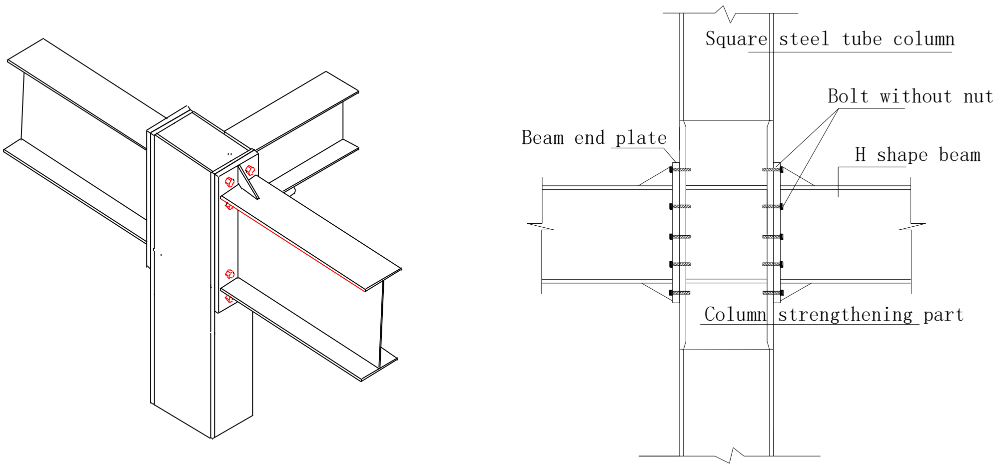


Fig. 1 New bolt node connection

## EXPERIMENTAL DESIGN

### 1 Design of the Specimen

A total of two beam and column connection node components are designed. Each component is in a middle-height column containing two adjacent floors and a half-across beam. New full bolt joint is adopted to connect steel beam and box column. All specimens are constructed by H200 x 100 x 6 x 10(mm) beams and 200 x 200 x 10 x 10(mm) box columns. In order to evaluate the influence of plate thickness on the seismic performance of the new structure, the wall thickness of JD-1 in the box column node area is set to $t$=16mm, and that of JD-2 is set to $t$=20mm. In order to reduce the influence of beam and column size on the connection characteristics, the width-thickness ratio of beam flange and web is 5 and 33.3 respectively, which can develop the whole plastic stress distribution. All steel plates are made of Q345 steel, and the properties of steel materials actually measured are shown in table 1. All bolts are made of M20 (diameter of 20mm) high-strength bolts, and the ultimate tensile strength of bolts is 1000MPa. Figure 2 shows the geometric shape and size of the specimen.

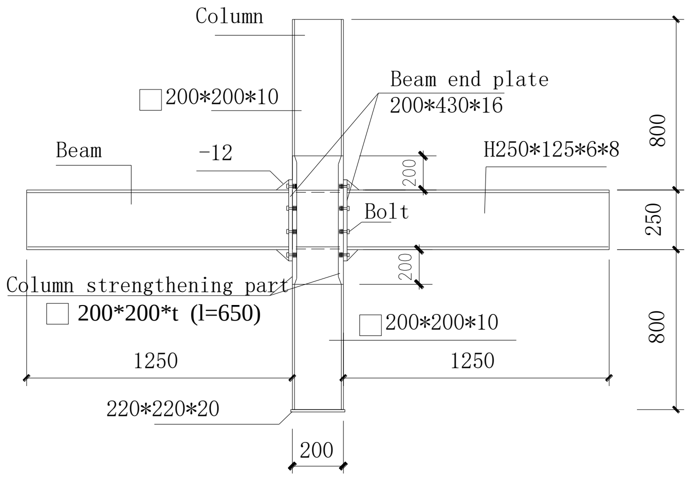


Fig. 2 Dimensions of specimens

**Table 1: Mechanical Properties of Steel**

| Specimen | Actual Thickness / mm | Elastic Modulus E/GPa | Yield strength $f$y/MPa | Tensile strength $f$u/MPa | Yield strain /10-3 | Elongation ΔL / % |
|---|---|---|---|---|---|---|
| 6mm | 5.6 | 203 | 363.33 | 461.67 | 1.74 | 23.3 |
| 10mm | 9.7 | 201 | 386.66 | 501.25 | 1.69 | 25.6 |
| 16mm | 15.8 | 207 | 372.92 | 508.37 | 1.78 | 26.7 |
| 20mm | 19.7 | 205 | 399.19 | 508.49 | 1.76 | 27.2 |

## 2 Loading Plan

The test was conducted at the civil engineering structure test center of Shihezi University. The test setup is shown in Figure 3. The upper and lower ends of the column and the left and right ends of the beam simulate the hinge joint. The circular load is applied on the top of the box column, the top of the column is controlled by a 500kN hydraulic jack, and the vertical axial pressure is 400kN. The entire test process is controlled by displacement. The initial displacement starts from 0mm with a displacement increment of 5mm in each stage. The load termination criteria include the following two aspects :(1) sudden failure of the specimen or sudden instability of component, resulting in unloadable load; (2) the load P at the column end reaches the limit value of $P_U$, which is lower than 85% of $P_U$[11].

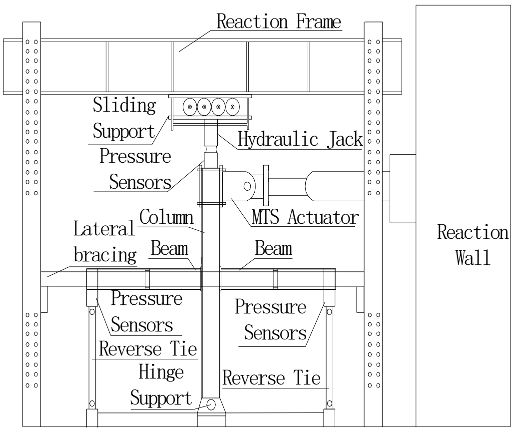


Fig. 3 Test setup

Fig. 4 Picture of test setup

## 3. Measuring Plan

A displacement meter is arranged at the bottom and top of the column to measure the displacement at the bottom and top of the column. Two displacement meters are arranged at the corner position of beam and column connection node to measure the rotation angle between beam and column. The strain gauge is attached to the flange 300mm from the column wall, and the strain gauges, 5 per set, is attached to the upper and lower flange of the beam and the web respectively to measure the yield of the beam. The schematic diagram of measurement point layout is shown in Figure 5.

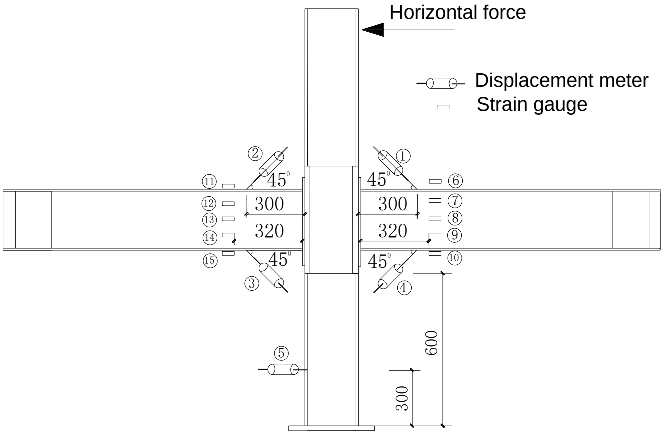


Fig. 5 Measurement layout

## EXPERIMENTAL PROCESS

For the specimen of JD-1, when the horizontal thrust load reaches 59kN and the displacement of the column top reaches 21.58mm, the load-displacement curve of the column end shows a turning point, indicating that the specimens reaches the yield load. At this stage, there is no obvious deformation and cracks in the weld; when the horizontal load reaches 114.42kn and the top displacement reaches 46mm, there will be crisp and subtle noises from the nodes; when the displacement of the column top reaches

74mm, the beam end plate bends. As the loading continues, the bending of the end plate and the gap between the flange and the end plate become more and more obvious; when the horizontal displacement of the top reaches 63mm, the first row of bolts under the lower part of the right end beam show signs of being pulled out. At the same time, the pushing force is significantly lower than the upper-level load; when the displacement of the column top reaches 77.6mm and the horizontal load reaches 139.6kN, the outermost bolt on the upper left side is pulled out; when the test was carried out to the next level of load, the right outermost bolt was pulled out, at this point, the load is 129.4kN and the top displacement reaches 73.6mm; when the top displacement reaches 100mm, the pushing and pulling force drops below 85% of the maximum load, and the loading stops. The failure form of the entire component is bolt failure, which indicates that when the thickness of the column wall at the node is thinner, the bolt failure is pulled-out failure. The component failure is shown in Figure 6.

(a) End plate deformation

(b) Bolt pulling out

Fig. 6 Failure of JD-1

For the specimen of JD-2, which is similar to that of JD-1 in the early stage. When the horizontal tension load reaches 159.8kN, the upper buckling deformation occurs at 10cm from the upper part of the flange of the right end beam. With the continuous load, both sides of the beam flange shows this phenomenon with a lasting development; when the horizontal displacement reaches 65mm and the horizontal thrust load is 163.4kN, there is brittle sound from the nodes, and the left end plate and the flange weld of the beam are torn apart. When the horizontal displacement reaches 63.6mm and the horizontal tension value is 149.3kN, the right upper end plate and the flange weld of the beam are torn apart, the upper flange of the left end is curved. When the horizontal displacement of the vertex reaches 95mm, the pushing force drops below 85% of the maximum load, the flange bends and becomes wavy, and the flange and the wall weld of the column are completely torn apart. In addition, there is no other phenomenon. When the loading stop, the bolts are well connected with no abnormality. Compared with JD-1, when the thickness of the column wall in the node area increases from 16mm to 20mm, the structure failure forms change from bolt pulling failure to beam bending failure. Therefore, as for such structure form, the thickness of the column wall in the node area has a great influence on the bolt bearing capacity. The failure of JD-2 is shown in Figure 7.

(a) Bending deformation

(b) Weld tearing

Fig. 7 Failure of JD-2

## TEST RESULTS AND DISCUSS

### 1 Hysteresis Characteristic

During the test, the hysteresis curves of the horizontal load and the horizontal displacement of the top of the column in JD-1 and JD-2 are shown in Figure 8. Since the thickness of the column wall is different, and the pushing and pulling force is reduced to less than 85% of the maximum load, the hysteresis curve of each specimen is significantly different. Through the hysteresis curves of the two specimen, it can be clearly seen that: (1) in the beginning of loading, the three specimens are in the elastic phase, and the hysteresis curve at this time is basically close to the straight line; (2) with the increase of the displacement, The hysteresis curve tends to develop from anti-S shape to fusiformis shape; (3) the hysteresis of JD-2 is better than the hysteretic loop of JD-1, because the energy dissipation capacity is weakened since the connection bolt is pulled out in JD-1; (4) The ultimate displacement and maximum load of JD-2 are larger than that of JD-1, indicating that the energy dissipation capacity and ductility of JD-2 are better than that of JD-1.

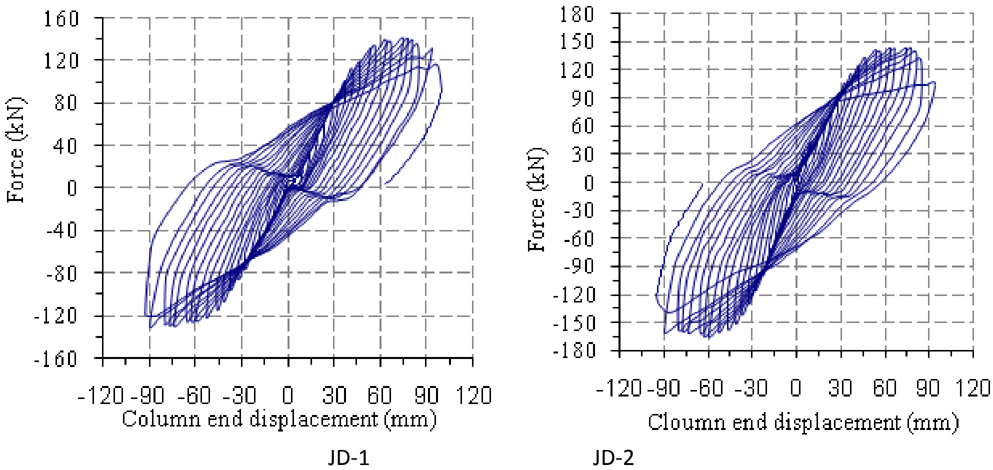


Fig. 8 Hysteretic curves of force-displacement relation

### 2 Skeleton Curves

The skeleton curves of specimen JD-1 and JD-2 are shown in Figure 9. Obviously, both of the two curves are straight lines in the elastic phase. The stiffness of specimen JD-2 is more larger than that of JD-1, indicating that when the thickness of the column plate in the joint area is larger, it is closer to the rigid connection. When the load at the column ends of JD-1 and JD-2 reaches 59.7kN and 68 kN respectively, the curve begins to bend and the elastic-plastic deformation is observed. The rigidity and ultimate bearing capacity of JD-2 is greater than that of JD-1, but when the ultimate displacement is reached, due to the welding fracture of the beam flange and end plate of JD-2, the specimen is invalid and the plastic deformation is not fully developed. The skeleton curve of the two specimens has obvious descending section with good ductility. The maximum bearing capacity of JD-1 is 139.5kN, and that of jJD-2 is 163.4kN, the maximum bearing capacity of JD-2 is 17.8% higher than that of JD-1. The positive and negative parts of the same curve are basically symmetric, indicating the same mechanical properties in the positive and negative directions.

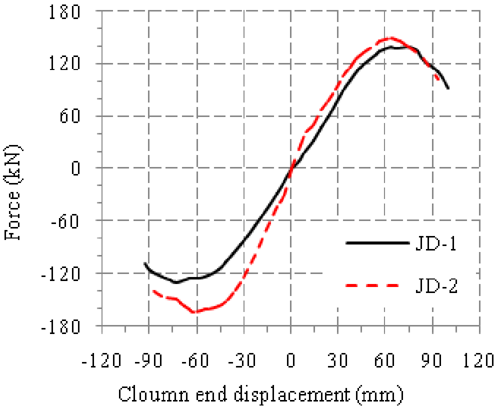


Fig. 9 Skeleton curves of force-displacement relation

## 3 Angle Calculation

Figure 10 is the arrangement of displacement meter diagram. The angle calculation formula for the value recorded by the displacement meter during the test is as follows:

$$\cos(90^0+\theta)=[(c+\Delta)^2-(a^2+b^2)]/2ab \tag{1}$$

The angle $\theta$ can be calculated.

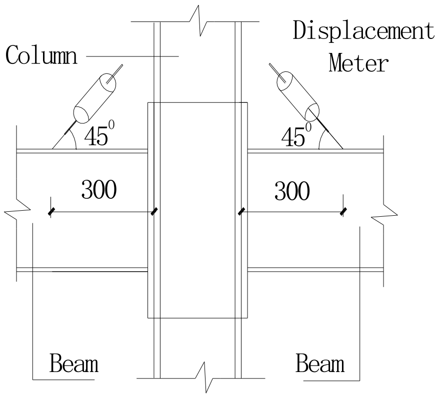


Fig. 10 Arrangement of displacement meter

Among them, $\theta$ is the node angle; $c$ is the initial side length of the triangular hypotenuse formed by the displacement meter, the column and the beam; $a$ is the initial side length of the triangular right angle side formed by the displacement meter, the column and the beam; $b$ is the initial side length of the other right angle of the triangle; $\Delta$ is the amount of change of the hypotenuse.

Finally, the bending moment angle curve shown in Figure 11 is obtained by calculation.

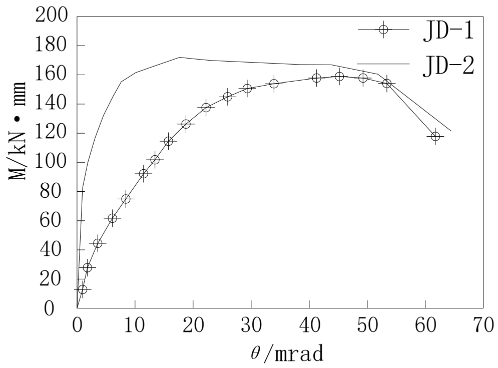


Fig. 11 Envelop curves of moment-rotation relation

It can be seen from the figure that JD-2 changes faster than JD-1 in the early stage. The bending moment value of JD-2 has reached the maximum value when $\theta$ is 18mrad, while JD-1 reaches the maximum value when $\theta$ is 45mrad. After the bending moment reached the maximum value, it will remain steady for a period of time before slowly declining. When the final failure was stopped, the values of JD-1 and JD-2 both are between 60~65mrad. It can be found that JD-2 is longer in the flat period.

## 4 Ductility and Energy Dissipation

Ductility refers to the inelastic deformation capacity calculated by hysteresis curve without significantly reducing the bearing capacity. The displacement ductility coefficient $\mu = \delta/\delta y$, where $\delta$ is the maximum horizontal displacement of the specimen at the time of failure[12, 13]. The hysteretic curve is in a region where it is closed in a cycle, it is an important index of seismic performance and describes the energy dissipation of the specimen. In this study, the equivalent damping coefficient He was used to describe the energy dissipation in the last hysteretic loop[14].The experimental results are shown in tables 2 and 3. Obviously, the ductility of JD-1 is poor, and the plastic development is not complete because the bolt is pulled out, indicating that the thickness of the column plate in the joint area has influences on the ductility. The ductility of JD-2 is completely developed, and the first yield of the beam significantly increased the ductility of the specimen. The equivalent viscous damping coefficient of JD-2 is greater than that of JD-1, and its energy dissipation is better than that of JD-1, indicating that the wall thickness of the joint area significantly increases the energy dissipation of the connector.

$$E = \frac{S_{\Delta ABC} + S_{\Delta CDA}}{S_{\Delta BOE} + S_{\Delta DOF}} \tag{2}$$

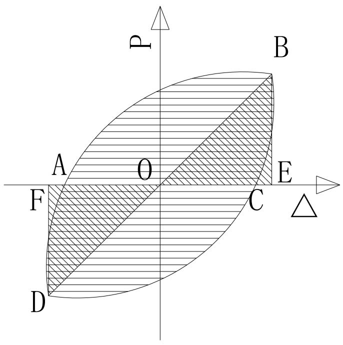


Fig. 12 Calculation diagram of energy dissipation

**Table 2: Analysis of Ductility**

| Specimen | Yield displacement /mm | Maximum displacement /mm | Ultimate displacement /mm | Displacement ductility ratio |
|---|---|---|---|---|
| JD-1 | 21.58 | 69.31 | 93.45 | 4.33 |
| JD-2 | 18.78 | 59.47 | 90.33 | 4.81 |

**Table 3: Coefficient of Energy Dissipation**

| Specimen | Yield load state /kN·mm | Maximum load state /kN·mm | limit load status /kN·mm | Coefficient of energy dissipation |
|---|---|---|---|---|
| -1 | 769.11 | 8910.55 | 15646.52 | 1.54 |
| JD-2 | 914.62 | 11328.35 | 16249.04 | 1.73 |

## 5. Stiffness Degradation

In order to reflect the stiffness degradation of different walls, taking the sum of the absolute value of positive and negative loads $P_i$ under reciprocating loads divided by the sum of the corresponding absolute value of positive and negative displacements $\Delta_i$ as the average stiffness $K_i$ of each stage of cyclic loading, as shown below:

$$K_i = \frac{|P_i| + |-P_i|}{|\Delta_i| + |-\Delta_i|} \tag{3}$$

Taking the average displacement as the horizontal coordinate and the average stiffness as the vertical coordinate, the stiffness degradation curve is shown in Figure 13 from which we can see that at the beginning of the test load, JD - 2 stiffness degradation is very obvious which is almost in a straight line down, while the stiffness of JD - 1 does not degrade sharp. With the increase of the displacement, the decline of the stiffness degradation of JD-2 curve is significantly slower, and the degradation trend of JD-1 and JD-2 is close at this stage. At the end of the test, the stiffness degradation of the two specimens is very close, indicating that the two specimens are failure at similar residual stiffness values.

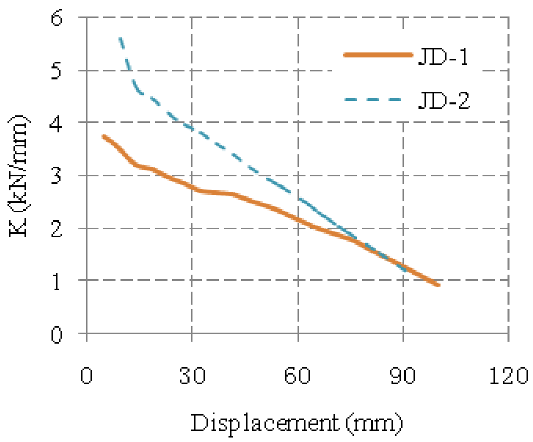


Fig. 13 Stiffness degradation curves

## CONCLUSION

Through the pseudo-static loading test and the analysis of the failure mechanism, hysteresis performance, stiffness degradation, energy consumption index, bending moment-rotation angle and ductility of the new bolt joints, the following conclusions can be obtained:

(1) The wall thickness of the column in the joint area has a significant impact on the failure form. When the wall thickness of the column is relatively thin, the bolt may be in a pulled-out failure.

(2) The ductility, energy consumption and bearing capacity of JD-2 are better than that of JD-1, indicating that the wall thickness of the column in the joint area has a significant influence on the seismic performance of the structure.

(3) The hysteretic performance of the two specimens is full, and the stiffness degenerates evenly and stably, indicating that the new all-bolt joint features with superior seismic performance and good energy consumption capacity.

## ACKNOWLEDGEMENTS

The authors would like to express their gratitude to the National Natural Science Foundation of China for their financial support of this study through grants No. 51368052.

## REFERENCES

1. Swanson1, James A. and Leon, Roberto T. (2000). “Bolted Steel Connections: Tests on T-stub Components”, Journal Structure Engineering, Vol. 126, pp. 50-56.
2. Popov, Egor P. and Takhirov, Shakhzod M. (2002). “Bolted Large Seismic Steel Beam-to-column Connections Part 1 : Experimental Study”, Engineering Structures, Vol. 24, pp. 1523-1534.
3. Ma, R.L., Yang, Y., Chen, Q.S. and Lu, L.X. (2009). “Seismic Performance Testing Study on High Strength Bolt Connections with Slotted Holes”, Journal Building Structure Vol. 30, No. 1, pp. 101-106 [in Chinese].

4. Gerami, M., Saberi, H., Saberi, V. and Daryan, A. Saedi (2011). "Cyclic Behavior of Bolted Connections with Different Arrangement of Bolts", Jounal Constr. Steel Res., Vol. 67, No. 4, pp. 690-705.
5. France, J.E., Davison, J.B. and Kirby, P.A. (1999). "Strength and Rotational Stiffness of Simple Connections to Tubular-columns using Flow Drill Connectors", Journal of Constructional Steel Research, Vol. 50, No. 1, pp. 15-34.
6. Ellison, S. and Tizani, W. (2004). "Behaviour of Blind Bolted Connections to Concrete Filled Hollow Sections", The Structual Engineer, Vol. 82, No. 22, pp. 16-17.
7. Gholami, M., Deylami, A. and Tehranizadeh, M. (2013). "Seismic Performance of Flange Plate Connections Between Steel Beams and Box Columns", Journal Constr. Steel Res., Vol. 84, pp. 36-48.
8. Wang, Z.Y. and Wang, Q.Y. (2016). "Yield and Ultimate Strengths Determination of a Blind Bolted Endplate Connection to Square Hollow Section Column", Engineering Structures, Vol. 111, pp. 345-369.
9. Zhenshan Tian, Mingsheng He and Kun Guo (2014). "Theoretical Analysis of New Bolt Force Characteristics", Progress in Steel Building Structures, Vol. 16, No. 1, pp. 1-6 [In Chinese].
10. Ming-sheng HE, Wang-zhi LI, Ze-feng HE and Li, LIU (2016). "Experimental Investigation of Bearing Capacity of New Type Unilateral Bolts", Journal of Lanzhou University of Technology, Vol. 42, No. 2, pp. 118-123 [In Chinese].
11. ANSI/AISC 341-05 (2005). "Seismic Provisions for Structural Steel Buildings", American Institute of Steel Construction, Chicago, Illinois, U.S.A.
12. Stoakes, C.D. and Fahnestock, L.A. (2011). "Cyclic Flexural Testing of Concentrically Braced Frame Beam–column Connections", Journal Structure Engineering, Vol. 137, No. 7, pp. 739-747.
13. Guo, B., Guo, Y.L., Liu, F., Li, M.G. and Chi, Y. (2006). "Research on Cyclic Behavior of Welded and Bolted Steel Frames", Journal Building Structure, Vol. 27, No. 2, pp. 47-56 [in Chinese].
14. Li, L.M., Chen, Z.H. and Li, N. (2007). "Experimental Study on Seismic Capability of Diaphragm—through Style beam–Column joint", Journal Earthqauke Eng. Vib., Vol. 27, No. 1, pp. 46-53 [In Chinese].